Scientific Research Publishing

International Journal of Geosciences, 2025, 16(6), 339-357
https://www.scirp.org/journal/ijg
ISSN Online: 2156-8367
ISSN Print: 2156-8359

Petrostructural and Microstructural Characterization of Granitoids from the Ziniare Region (Central Burkina Faso, West Africa)

Saga Sawadogo[1*], Abraham Seydoux Traore[1], Oussény Sourgou[2]

[1]Geosciences and Environment Laboratory, Department of Earth Sciences, Joseph KI-ZERBO University, Ouagadougou, Burkina Faso
[2]University Center of Manga, Norbert ZONGO University, Koudougou, Burkina Faso
Email: *sawadsaga@gmail.com

How to cite this paper: Sawadogo, S., Traore, A.S. and Sourgou, O. (2025) Petrostructural and Microstructural Characterization of Granitoids from the Ziniare Region (Central Burkina Faso, West Africa). *International Journal of Geosciences*, **16**, 339-357.
https://doi.org/10.4236/ijg.2025.166017

Received: May 11, 2025
Accepted: June 14, 2025
Published: June 17, 2025

Abstract

The Ziniare region is mainly made up of volcano-sedimentary and granitoid formations: the highly altered volcano-sedimentary formations are shales corresponding to the relics of the Birimian furrows, whose general orientation varies from north-south (N-S) to north-east-south-west (NE-SW). This structure is the result of regional shortening from east-west (E-W) to north-west-south-east (NW-SE), associated with the first phase of deformation (D1), which was ductile in nature. The granitoids present in the region can be divided into two groups: first-generation granitoids, belonging to the TTG series (tonalite-trondhjemite-granodiorite) and second-generation granitoids, represented in particular by the Ziniaré granitic pluton. The first-generation granitoids are oriented and affected by a second phase of deformation (D2), with a mean direction of N40. This deformation, marked by sinister shearing, is part of a tectonic continuum ranging from low-temperature to high-temperature conditions. It led to the development of characteristic tectonic structures such as sigmoidal cracks and pressure shadows, reflecting the intensity of the stresses exerted. The microstructures observed in these granitoids reflect a post-magmatic evolution acquired during this D2 phase. The D2 phase, which is predominantly east-west (NE-SW), may or may not have been taken over locally by a third phase of deformation (D3), marked by dextral shearing. In some areas, this phase affected the Ziniaré granitic pluton. However, on the whole, the microstructures observed in this pluton are mainly of magmatic origin, reflecting emplacement in a weakly deformed regime.

Keywords

Deformation, Structure, Granitoid, Shear, Phase

1. Introduction

The West African Craton is essentially made up of the Reguibat Ridge to the north and the Man/Leo Ridge to the south [1] [2]. The Man Ridge comprises an Archean (3.00 - 2.50 Ga) or Kenema-Man domain corresponding to the core of the ridge and a Palaeoproterozoic or Baoulé-Mossi domain, representing the juvenile part [3]-[6] (**Figure 1**). The Baoulé-Mossi domain is composed of granites, suites of TTG (Tonalite-Trondjhemite-Granodiorite) and belts of Birimian greenstone [7] [8].

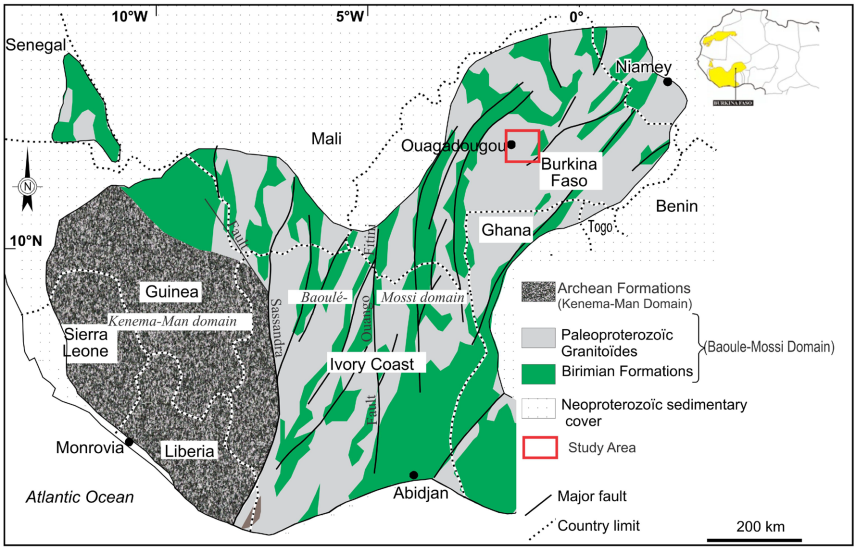

Figure 1. Simplified geological map of the Man/Leo Ridge [14].

The Birimian greenstone belts comprise elongated sequences of metavolcanic and metavolcanosedimentary rocks that are Birimian trenches. These are essentially metabasalts, metaandesites and volcanic sediments metamorphosed in the Eburnian [9]-[12]. The volcanic activity that gave rise to these rocks occurred around 2.40 Ga and lasted locally until 2.10 Ga [13]-[15].

Numerous authors have demonstrated that lithostratigraphic succession first favours the emplacement of suites of TTGs commonly known as first-generation granitoids [16]-[18]. These TTGs result from intense plutonic activity before magmatism progressively evolves towards more differentiated terms (potassic granites and alkaline syenites) or second-generation granitoids [19]-[21]. After this magmatic accretion of juvenile crust, the Eburnian orogenic cycle led to the tectonic assembly of the Archean and the various Palaeoproterozoic domains between 2.15 and 2.08 Ga [14] [22]-[25].

This orogenic cycle coincides with the establishment of vast granitoid domains. The most undifferentiated terms or first generation granitoids or TTGs are the oldest granitoids and are known as rocks that are most often structured by field observation. However, second-generation granitoids are generally poorly structured and appear to be isotropic when observed in the field. By examining microstructures, it is possible to characterise the rheological state of the material during or after its emplacement, and the Magnetic Susceptibility Anisotropy (MSA) approach will reveal structures that would not have been apparent during field observation.

The aim of this study is to contribute, through petrographic, microstructural and structural studies, to a better understanding of the geological processes that led to the emplacement of the granitoids in the central region.

2. Regional Geological Context

Geological reconnaissance work has been carried out in the central part of Burkina Faso, and an extensive mapping campaign covered the area in 2003 [17] [20].

Like the other regions of the Baoulé-Mossi domain, and on the basis of the work already carried out, the study area comprises greenstone belts within which metavolcanic rocks (metabasalts, metaandesites, etc.) and, to a lesser extent, metaplutonic rocks (metagabbros, metadiorites, etc.) and metasedimentary rocks (schists, metapelites, etc.) are found. This schistose series also contains intercalations of intermediate to acid volcanics, including a rhyolitic tuff dated at 2238 ± 5 Ma, corresponding to the oldest age obtained to date in Burkina Faso and indirectly confirming that amphibolitised basalts are the oldest rocks in Burkina Faso [20].

All these formations are affected by greenschist to amphibolite facies metamorphism, with hydrothermal circulation superimposed in places.

Within the Goren arc, these formations develop a schistosity (S1) that is the result of regional NW-SE shortening. This S1 is interpreted as being the result of the first deformation phase of the Eburnian orogeny and corresponds broadly to phase D1 [17] [20].

The greenstone belt formations corresponding to the Goren belt are cut by two generations of granitoids. Granitoids with a geochemical signature close to that of the Archean TTGs (Tonalites, Trondhjemites and Granodiorites) [17] [21] [26] [27] or Andean adakites [2] constitute the first generation of granitoids that cut the greenstone belts, especially in the Ouagadougou area.

The emplacement of these granitoids produced a halo of contact metamorphism in the surrounding formations [28] [29]. The first-generation granitoids and greenstone belts are intersected by a second generation of granitoids. The TTG granitoids are generally more or less clearly banded at field scale, whereas the second-generation granitoids are generally poorly structured. In terms of mineralogical composition, TTG granitoids generally contain both biotite and amphibole as ferromagnesian minerals, whereas second-generation granitoids generally

have biotite as the only ferromagnesian mineral.

In this central part of Burkina Faso, which belongs to the Ouagadougou sheet [17], it is these granitoids that are the focus of this article (**Figure 2**).

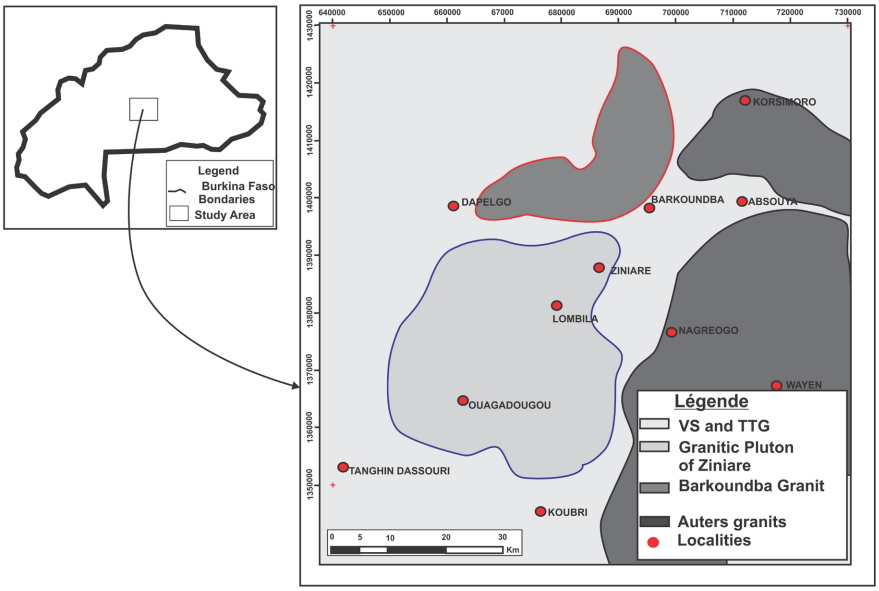

Figure 2. Geological map of the study area (extract from the 1/2,000,000 geological map of Burkina Faso [17].

3. Methodology

For this study, the methodology consisted of documentation, fieldwork, laboratory work and interpretation of satellite images and data.

The literature review provided an overview of previous and ongoing work in the study area.

For the field work, sampling was carried out using the ASM approach, where it is common practice to sample regularly and evenly across the pluton [26] [29]-[31].

Laboratory work consisted of making thin sections for detailed petrographic descriptions and for examining microstructures.

4. Results

4.1. Petrographic Characteristics

In the study area, the geological formations encountered are volcanosedimentary rocks and granitoids.

The volcanosedimentary rocks belong to the Goren arc, which borders the northern part of the study area (**Figure 3(a)**). Very discrete and weathered outcrops were observed in the south-eastern part of the study area. Their highly weathered nature means that no minerals can be seen in the outcrop and it was not possible to make thin sections. They are oriented N-S to NNE-SSW in the same direction as the shear corridor (**Figure 3(b)**).

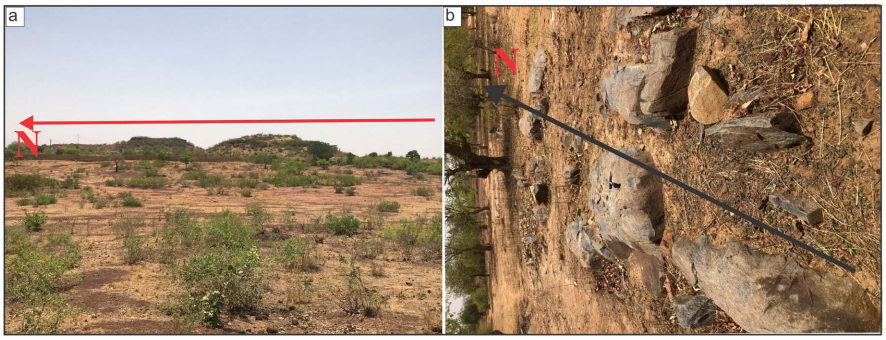

Figure 3. Volcano-sedimentary belt rocks and shear corridor, (a) Birimian trenches, (b) Shear corridor with alternating TTG and volcano-sedimentary rocks.

The granitoids in the Ziniaré region consist mainly of first-generation or TTG granitoids and second-generation granitoids, including the Ziniaré Granite Pluton (PGZ).

The first-generation granitoids are essentially represented by tonalitic facies.

At outcrop, the tonalitic facies has a grey colour with a grainy texture and minerals such as amphiboles, biotite, plagioclases, potassium feldspars and quartz. These minerals show preferential NNE to NE shear orientations. Comagmatic enclaves have also been observed on these tonalites (**Figure 4(a)**, **Figure 4(b)**).

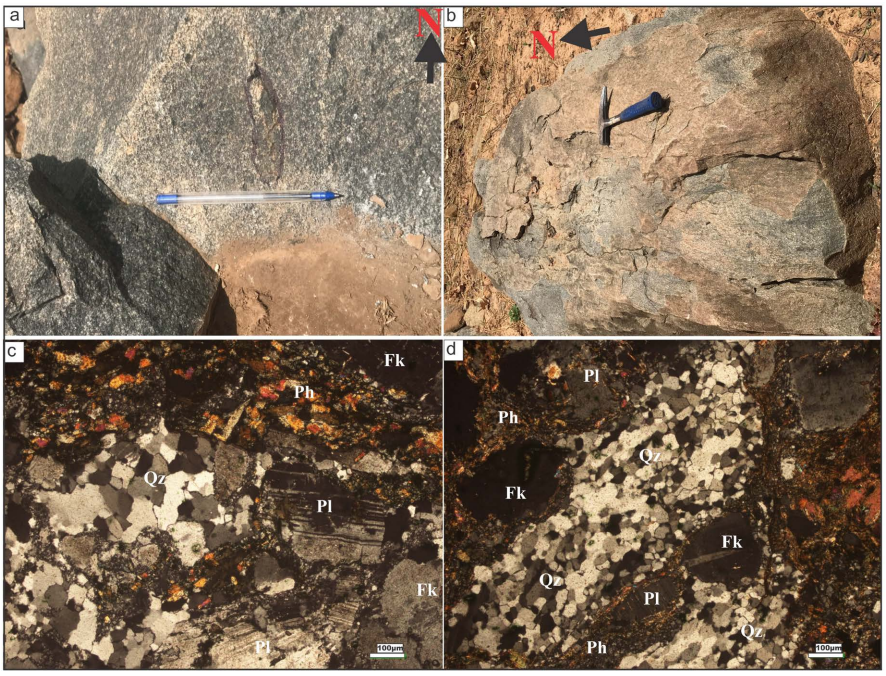

Figure 4. Tonalitic facies, (a) Massive tonalite rift with enclave, (b) Foliated tonalite rift, (c), (d): microphotograph of tonalitic facies. Ph: Amphibole and biotite philites, Pl: Plagioclase, Fk: Potassium feldspar, Qz: Quartz.

Contacts between the tonalitic facies and the PGZ are also observed in places. These relationships show that it is cut by the PGZ. This is the close host of the PGZ. Contacts between the tonalitic facies and the volcano-sediments are also ob-

served. The latter are cut by the tonalitic facies.

Microscopically, the rock consists mainly of amphibole, biotite, plagioclase, potassium feldspar and quartz. Amphibole is usually stable and combines with biotite to form streaks of philite minerals (Figure 4(b), Figure 4(c)). Biotite is altered to chlorite.

The plagioclases are macerated and form zonations that indicate a differentiation between the core and the periphery. The potassium feldspars are perthitic and poecilitic (Figure 4(c), Figure 4(d)). Quartz has a rolling extinction and is recrystallised with more or less lobed sub-grains (Figure 4(c), Figure 4(d)).

Secondary minerals include sphene, allanite-type epidote and opaque zircon. The alteration minerals observed are myrmekite, chlorite and white micas.

The PGZ consists of the Barkoundba granitic facies (Figure 5(a)) and the Ziniaré granitic facies (Figure 5(b)).

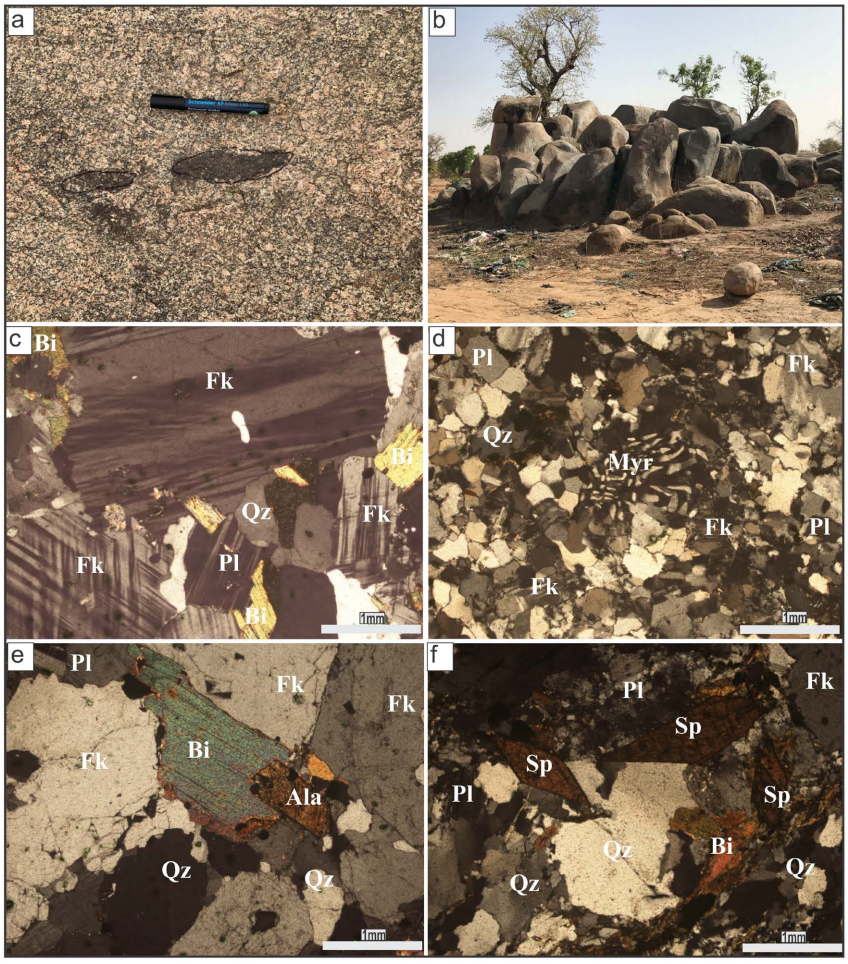

Figure 5. Macroscopic and microscopic illustrations of second-generation grantoids, (a) Macrophotograph of Barkoundba facies, (b) Macrophotograph of Ziniaré facies, (c) Microphotograph of Barkoundba facies with perthitic potassic feldspars, (d) Microphotograph of the Ziniaré facies with myrmekite, (e) Microphotograph of the Barkoundba facies with allanite, (f) Microphotograph of the middle facies with sphene. Bi: Biotite; Pl: Plagioclase, Fk: Potassium feldspar, Myr: Myrmekite, Sp: Sphene, Ala: Alanite.

The Barkoundba facies is a homogeneous coarse-grained granitic facies that outcrops quite acceptably. Occasionally, the facies outcrops discretely and more often it is very weathered. This facies is fairly homogeneous and has a grey colour on outcrop with plagioclase and feldspar phenocrysts.

Macroscopic observation reveals biotite, plagioclase, potassium feldspar and quartz. Biotite is more or less stable. The plagioclases are macerated and the potassium feldspars are poecilitic (**Figure 5(c)**). Accessory minerals include sphene, myrmekite and allanite (**Figure 5(e)**). Two generations of fractures are observed on this facies. An N-S oriented F1 fracture and an E-W oriented F2 fracture. These fractures are discrete and are not found everywhere. Comagmatic enclaves are also very common. These enclaves are altered to leave pot-like impressions (**Figure 5(a)**).

The Ziniaré facies sometimes outcrops over more than 2 km long and 500 m wide, with a medium-grained, grainy texture. The minerals are barely visible to the eye in the case of the fine-grained sub-facies. The main minerals observed are biotite, plagioclase, feldspar and quartz. Accessory minerals are myrmekite, sphene and allanite (**Figure 5(d)**, **Figure 5(f)**). Microscopically, biotite is in the form of more or less stable lamellae. The plagioclases are macerated and the potassium feldspars are poecilitic and perthitic. The quartz is lobed.

It should be noted that in places the two facies outcrop concomitantly. A fine facies next to a coarse Barkoundba facies which appears to be older in view of the criteria observed, including schistosity and fractures.

4.2. Microstructural Analysis

Microscopic observation of the slides revealed four types of microstructure. These are deformation microstructures in the magmatic state (EM), submagmatic microstructures (SUB), microstructures in the solid state HT (HT) or BT (BT) and incipient orthogneissification microstructures (ORT). These microstructures are summarised in **Table 1**.

Table 1. PGZ microstructures.

Sites	Villages	X (m)	Y (m)	Z (m)	Microstructures
OU0038A	Pazani	654,322	1,375,457	302	BT
OU0038B	Pazani	654,322	1,375,457	302	BT
OU0042A	KCB	683,870	1,383,042	307	BT
OU0042B	KCB	683,870	1,383,042	307	BT
OU0043A	Tanlorgho	681,062	1,382,883	300	BT
OU0043B	Tanlorgho	681,062	1,382,883	300	BT
OU0044A	Nomgande	679,227	1,381,745	302	BT
OU0044B	Nomgande	679,227	1,381,745	302	BT
OU0045A	Tangporin	666,795	1,399,192	314	BT

Continued

OU0045B	Tangporin	666,795	1,399,192	314	BT
OU001A	Saaba sud (Nagrin)	678,682	1,371,229	268	BT
OU002B	Yargo	679,172	1,363,024	290	BT
OU002C		679,172	1,363,024		BT
0U003A	Nakamtenga	680,706	1,354,392	296	BT
OU004A	Benongo	676,709	1,357,672	310	BT
OU004B		676,709	1,357,672	310	BT
OU005A	Mogtedo	674,959	1,357,141	317	BT
OU0053C	Ziniaré Natenga	687,083	1,391,340		BT
OU0056A	Site Laongo	686,424	1,386,581		BT
OU056B	Site Laongo	686,424	1,386,581		BT
OU0025A	Echa	681,883	1,387,914	298	EM
OU0025B	Echa	681,883	1,387,914	298	EM
OU0026A	Echa 11 Decembre	683,595	1,387,557	329	EM
OU0026B	Echa 11 Decembre	683,595	1,387,557	329	EM
OU0027A		679,238	1,386,841	300	EM
OU0027B		679,238	1,386,841	300	EM
OU0028A	Bagrin	677,614	1,385,518	300	EM
OU0028B	Bagrin	677,614	1,385,518	300	EM
OU0029A	Zongo	674,887	1,387,534	305	EM
OU0029B	Zongo	674,887	1,387,534	305	EM
OU0030A	Zongo	674,590	1,387,066	305	EM
OU0030B	Zongo	674,590	1,387,066	305	EM
OU0031A	Zagbega	680,564	1,391,488	314	EM
OU0031B	Zagbega	680,564	1,391,488	314	EM
OU0032A	Namassa (TT mining)	678,325	1,391,075	309	EM
OU0032B	Namassa (TT mining)	678,325	1,391,075	309	EM
OU0033A	Zongo Est	673,745	1,387,656	306	EM
OU0033B	Zongo Est	673,745	1,387,656	306	EM
OU0034A	Bagrin	680,167	1,386,830	299	EM
OU0034B	Bagrin	673,745	1,387,656	306	EM
OU0035A	Bagrin	679,463	1,385,961	306	EM
OU0035B	Bagrin	679,463	1,385,961	306	EM
OU0036A	Mandibga	677,849	13,844,482	298	EM
OU0036B	Mandibga	677,849	13,844,482	298	EM
OU0037A	Loumbila	674,219	1,381,022	269	EM
OU0039A	Kokin	660,221	1,388,569	314	EM
OU0039B	Kokin	660,221	1,388,569	314	EM

Continued

OU0040A	Bagrin	674,407	1,388,009	303	EM
OU0040B	Bagrin	674,407	1,388,009	303	EM
OU0041A	Kouanda	679,252	1,381,584	298	EM
OU0041B	Kouanda	679,252	1,381,584	298	EM
OU0053A	Ziniaré Natenga	687,083	1,391,340		EM
OU0053A	Ziniaré Natenga	687,083	1,391,340		EM
OU0057A	Zagbega (ziniaré)	684,073	1,391,022		EM
OU0059A	Pousgziga	683,990	1,389,831		EM
OU0061A	Koala 2	687,178	1,370,279		EM
OU0062A	Forert Classé de Gonssin	682,848	1,368,501		EM
OU0076A	Barkoundba	691,662	1,399,673		HT
OU0079A	Zegdsé	692,083	1,401,796		HT
OU0080A	Bissiga	696,709	1,404,712		HT
OU0081A	Bissiga	695,783	1,402,981		HT
OU0082A	Bissiga	697,576	1,404,109		HT
OU0083A	Zitenga	693,789	1,402,529		HT
OU0084A	Lemnogo	693,743	1,400,423		HT
OU0085A	Tibin	689,651	1,394,436		HT
OU0086A	Soulgo	688,432	1,392,399		HT
OU0052B	Ziniaré	690,424	1,397,565		ORT
OU0052B	Ziniaré	690,424	1,397,565		ORT
OU0055A	Seba	686,589	1,387,352		ORT
OU0055B	Seba	686,589	1,387,352		ORT
OU0075A	Nakamtenga	690,362	1,397,406		ORT
OU0077A	Napalga	690,377	1,402,762		ORT
OU0078A	Bissiga	694,279	1,404,399		ORT
OU0060A	Koala	688,110	1,371,648		SUB

Magmatic microstructures are more common in the PGZ. They are characterised by minerals free of any deformation (Figure 6(a)). Biotites in more or less stable lamellae. Plagioclases are stable and altered. The potassium feldspars are perthitic and poecilitic, while the quartz has a rolling extinction.

Sub-magmatic microstructures are characterised by fissured, quartz-filled plagioclases (Figure 6(b)).

Solid-state deformation microstructures are observed in the tonalites, the Barkoundba Granite Pluton and the edges of the Ziniaré Granite Pluton. It may be Low Temperature (LT) or High Temperature (HT). At BT, the plagioclases and biotites undergo ductile and plastic deformation, while the quartz recrystallises

into sub-grains with poorly restored contours (Figure 6(c)). At HT the plagioclases are flexured while the biotites are crumpled and sometimes in the form of trains (Figure 6(d), Figure 6(e)). Quartz recrystallises with well-contoured subgrains.

For incipient orthogneissification microstructures, in addition to the behaviour of minerals in the HT solid state, certain minerals such as quartz, plagioclases and potassic feldspars individualise in the form of phenoblasts, sometimes with shadows of recrystallisation pressure (Figure 6(f)). These microstructures are observed on the Barkoundba granitic pluton. The intensity of the deformation is such that the minerals are organised into light and dark beds. The biotites and amphiboles are in the form of trains that make up the dark beds. Quartz is recrystallised in a continuum of deformation from High Temperature (HT) to Low Temperature (BT).

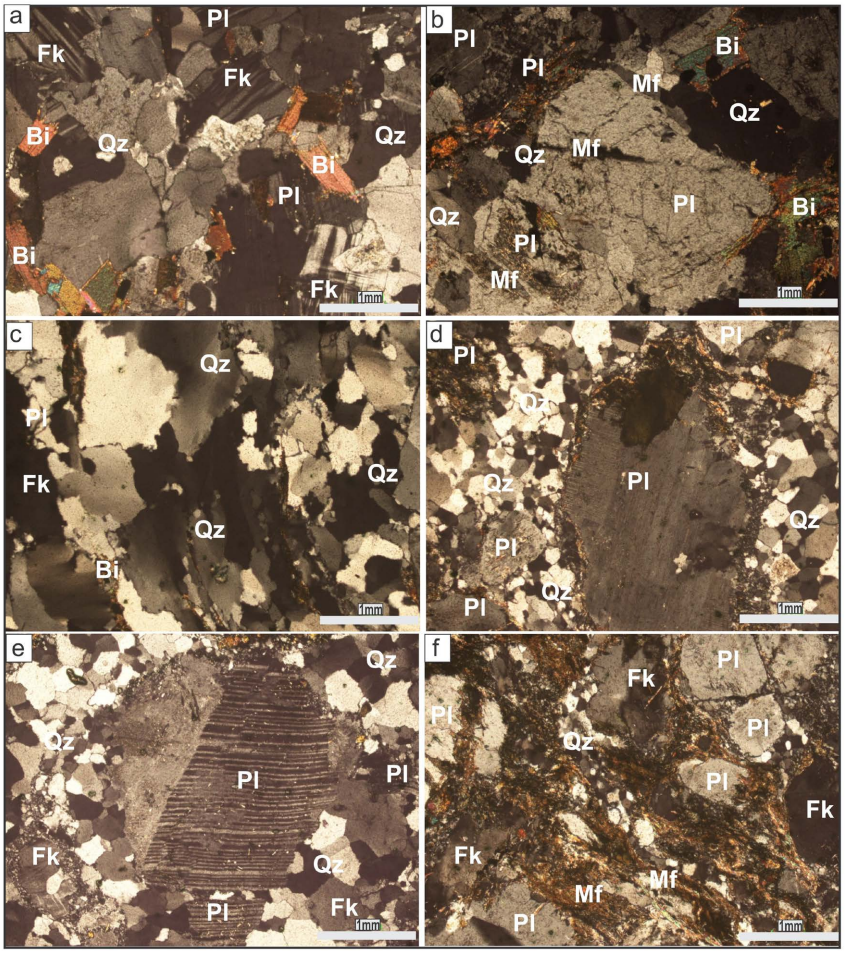

Figure 6. The different types of microstructures, (a) Magmatic state, (b) Submagmatic state, (c) BT solid state with subgrain recrystallised quartz with poorly restored contours, (d) HT solid state with subgrain recrystallised quartz with well restored contours, (e) HT solid state with flexural plagioclase, (f) Incipient orthogneissification with pressure shadows. Bi: Biotite; Pl: Plagioclase, Fk: Potassium feldspar, Myr: Myrmekite, Qz: Quartz, Mf: microfracture.

4.3. Pluton Boundaries, Structures and Deformation

The study area was processed using Landsat 8 satellite imagery in colour composition 7-6-5 (Figure 7(a)), a colour composition suitable for identifying lithological features. The result of this processing was superimposed on data from rock samples after observation of thin sections and on microstructural data.

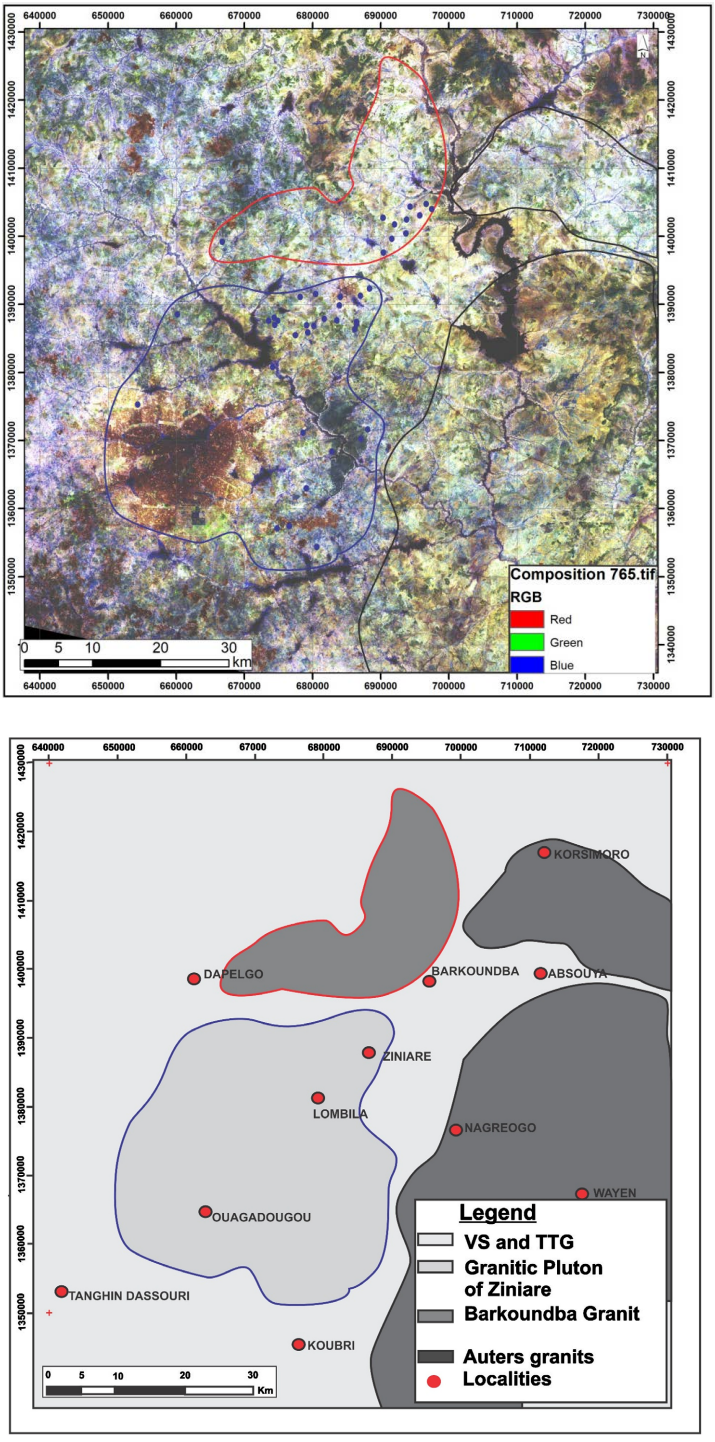

Figure 7. Interpretation of satellite imagery and the limits of pluton.

We found that the two facies are distinct in terms of petrography, microstructure and panchromatic signature. This ensemble was then superimposed on the 1:200,000 Ouagadougou geological map to better position the regional shear zones. Three regional shear corridors stand out. These are the Tanghin Dassouri-Ouagadougou-Ziniaré shear corridor, the Koubri-Nagréogo shear corridor and the Dapelgo shear corridor.

All the interpreted data were used to propose more acceptable boundaries for the two plutons at Barkoudba and Ziniaré (**Figure 7(b)**). Final processing produced a lithostructural map of the study area (**Figure 8**).

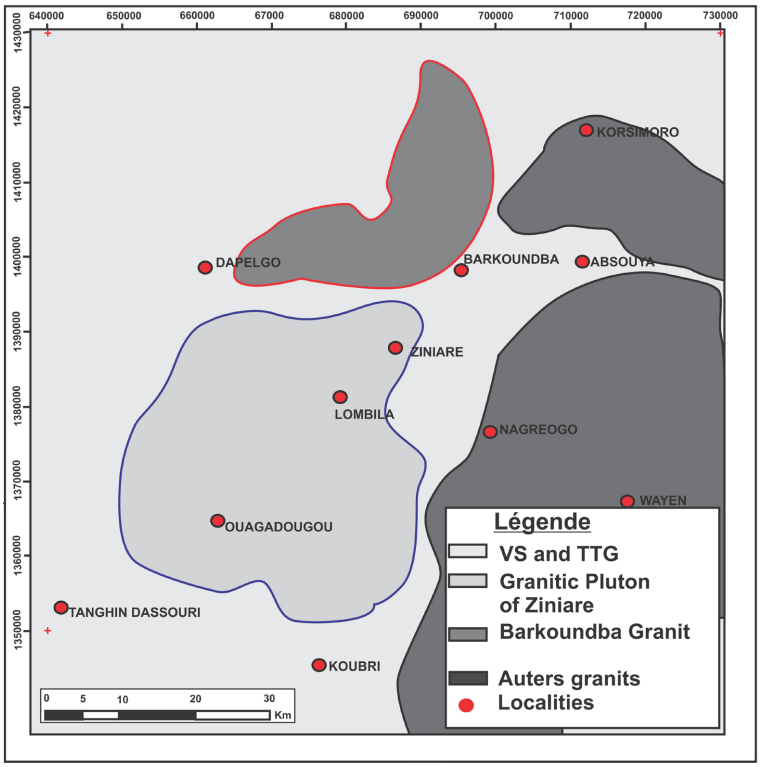

Figure 8. Lithostructural map of the study area.

In the field, quartz veins are rare in the Barkoundba granite. Quartz veins, on the other hand, are found both on the Ziniaré granite and in the tonalites. Three generations of quartz veins have been observed. These are veins V1 with a mean orientation N40, V2 with a mean orientation N60 and V3 with a mean orientation E-W.

The cracks are found in the Ziniaré granite, particularly in the south-eastern part, and are oriented N-S. These are tension cracks, which are oriented in the same direction as the enclaves (**Figure 9(a)**), and sigmoidal cracks, which reflect the effects of shearing (**Figure 9(b)**).

Three shear zones were visibly observed in the field (**Figure 9(c)**, **Figure 9(d)**). A shear zone oriented N40, observed in the central part corresponding to the passage of the Tanghin Dassouri-Ouagadougou-Ziniaré shear zone. A second N20-

trending shear zone corresponding to the passage of the Koubri-Nagréogo shear zone and a third E-W shear zone observed at Namassa and to the south of Ziniaré. The third shear zone is more recent and cuts across the Koubri-Nagréogo shear zone.

Some granitoids, such as the TTGs, show foliation. The minerals are oriented in the direction of the shear zone.

Interpretation of the deformation structures observed in the field suggests three deformation phases D1, D2 and D3 in this central part of Burkina Faso.

D1 characterises the alignment of the Birimian furrows observed in the eastern and northern parts of the study area. This phase of early, probably ductile, deformation has been interpreted as regional E-W to NW-SE shortening. The end of this phase coincides with the emplacement of the TTGs.

This D1 was taken over by the sinister D2 (**Figure 9(b)**), which developed cracks and then sigmoidal cracks in a continuum of deformation, as observed in the field (**Figure 9(b)**). It is semi-ductile and developed the Dapelgo, Tanghin Dassouri-Ouagadougou-Ziniaré and Koubri-Nagréogo shear zones.

In places, D3 overprinted the D2 deformation phase. The fractures developed by this latter dextral phase are oriented E-W and coincide with the Laongo shear zone (**Figure 9(a)**).

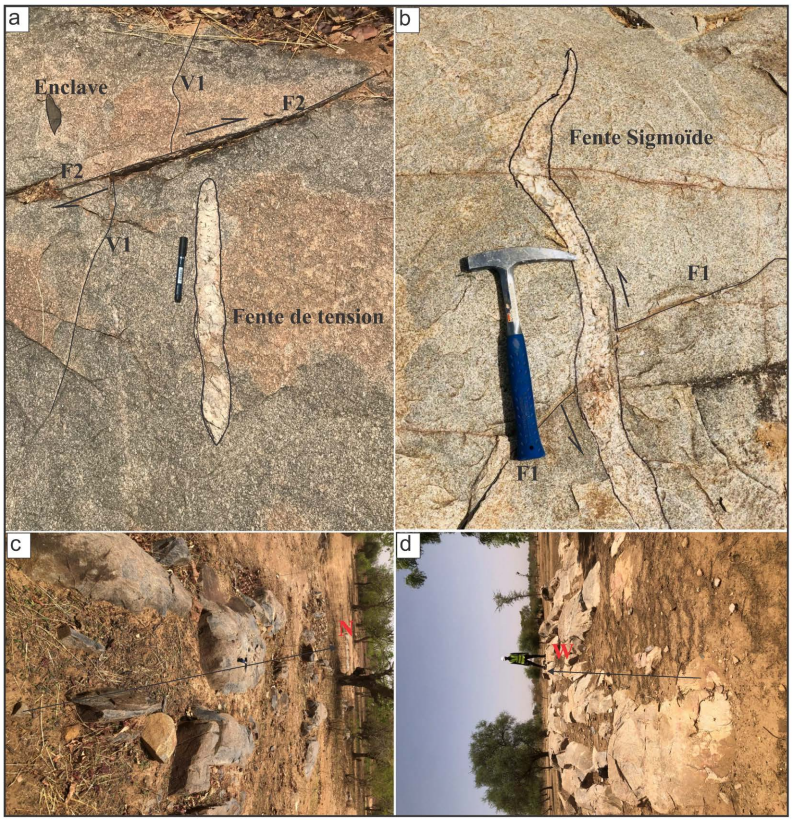

Figure 9. Structures and deformation phases, (a) D3 dextral shear zone with tension crack, (b) D1 sinister shear zone with sigmoidal crack, (c) Passage of the Koubri-Nagreogo shear zone, d-Passage of the E-W oriented D3 shear zone.

Overall, the passage of these shear zones within the plutons is highlighted by low-temperature solid-state deformation microstructures (Figure 10, Figure 11).

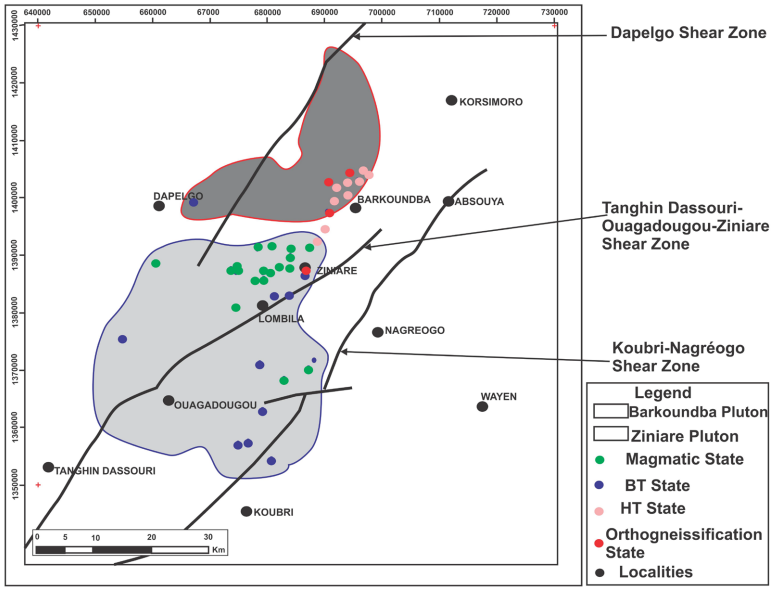

Figure 10. Microstructures and shear zones.

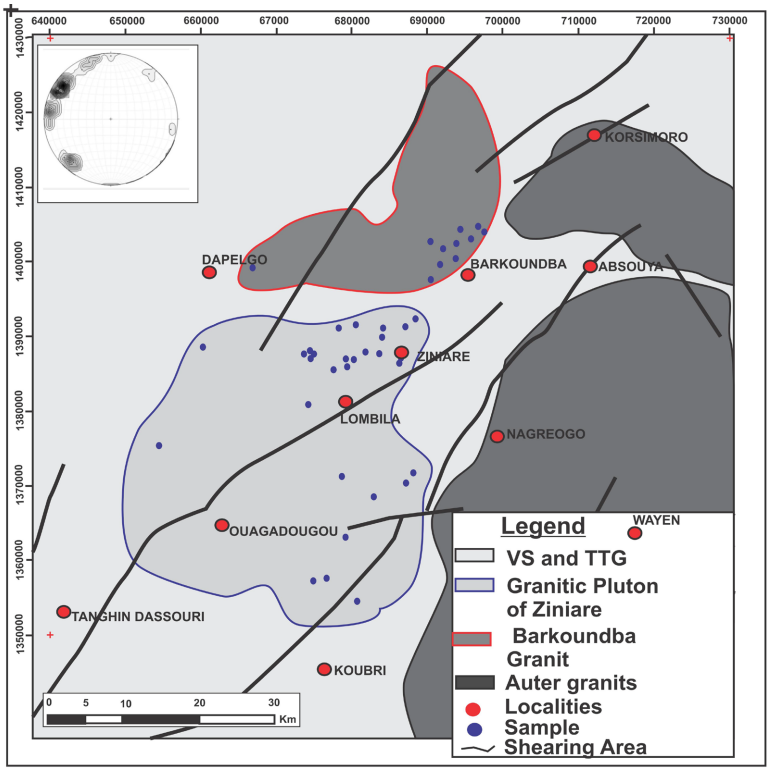

Figure 11. Structural map.

5. Discussion

The N-S to NE-SE alignment due to the E-W to NW-SE regional shortening of

the Birimian trenches is known in the West African Palaeoproterozoic terrains of the Léo Dorsal [4] [13] [19] [32]-[34] and elsewhere in Guinea [35], Morocco [36] [37], Senegal [38] [39], Ghana [4] [5], Niger [40] and Burkina Faso [16] [21] [41] [42]. These same forms of green belt are found in the study area and correspond to the oldest formations in this central part of Burkina. They define the Goren arc [43] and border the northern and north-western parts of the study area [20] [44].

The shaping of these Birimian furrows is the result of a regional E-W to NW-SE shortening corresponding to deformation phase D1. It is ductile and has developed S1 schistosity when visible in the field or not, as in the case of our study area [45].

This phase of deformation was partially or totally delayed, as was the case in our study area, by the second phase of deformation, D2, which is ductile and brittle and played in a sinister direction. This sinister play of D2 is consistent with the plays of the major shear zones that exist within in the Palaeoproterozoic domain, such as the Tiébélé-Dori-Markoye fault [42] [43] [46], the Sassandra fault in Côte d'Ivoire [13] and the Senegal-Malian fault [38].

In the case of our study area, this D2 phase affected first-generation granitoids whose deformation markers are visible in the field, such as fractures, cracks and foliations. This played a fundamental role in the redistribution of magmatic-state microstructures to high-temperature or low-temperature solid-state microstructures, sometimes with incipient orthogneissification. By deduction, these microstructures were acquired after the massif had cooled completely. This reflects the rheological state of the material, which could be characterised by examining the microstructures [47]. This same approach has been used to characterise granitoids in NE Benin [42] [48] and Burkina Faso [29].

Subsequently, the D3, which is dextral, took over from the D2 in places. It is brittle and of low intensity in the sense that, despite its effects, the Ziniaré granite pluton remains undeformed with microstructures of a dominant magmatic state within the study area. The transition from D3 is nevertheless marked by an alignment of low-temperature solid-state microstructures.

In the northern part of the study area, four deformation phases have been identified, of which D1-x, described by Tangaen, is ante-Birimian and phases D1, D2 and D3 are Birimian [42]. In addition, in the southern part of the study area, near the Kiaka gold deposit, four deformation phases have been identified, of which D4 is very localised and the other phases are similar to those in our study area [46].

The three phases of deformation identified and proposed in this central part of Burkina Faso are consistent with the evolution of deformation in other regions studied by certain authors, with which a fourth phase, whether local or not, is associated [6] [35] [40] [44].

6. Conclusions

The methodological approach adopted has enabled us to distinguish two major lithological groups in the study area: volcano-sedimentary rocks and granitoids.

The former are highly altered and are interpreted as volcano-sedimentary schists, the relics of which are the elongated structures of the birimian furrows. The latter are inherited from the D1 deformation phase, characterised by ductile behaviour. The granitoids can be divided into two generations. The first is represented by TTG-type granitoids (Tonalite-Trondhjemite-Granodiorite), while the second includes later intrusions such as PGZiniaré. The microstructural study revealed the presence of four types of microstructure, ranging from magmatic state structures to incipient orthogneissification structures, via submagmatic states and structures acquired in the solid state, either at high or low temperature.

Microstructural analysis shows that the PGZ is dominated by magmatic-state microstructures, suggesting complete crystallisation of the magma without major subsequent structural alteration. In contrast, the Barkoundba granitic pluton is dominated by incipient orthogneissification microstructures, indicating significant deformation associated with the D2 phase. This ductile to brittle phase contributed to the gradual transformation of the magmatic texture towards a gneissic texture.

Interpretation of the structures, based on a relative chronology, has enabled three major successive deformation phases to be reconstructed: an initial ductile D1 phase, a marked sinister D2 phase, and a late dextral D3 phase, of weaker intensity, but locally identifiable by the alignment of low-temperature solid-state microstructures.

Acknowledgements

This work is a contribution to the characterisation of granitoids from the Ziniaré region, which is located in central Burkina Faso.

We would like to thank the head of the Geosciences and Environment Laboratory (LaGE) for making the slides and observing them under the microscope, and the Burkina Faso Bureau of Mines and Geology for drilling the samples.

Conflicts of Interest

The authors declare no conflicts of interest regarding the publication of this paper.

References

[1] Abouchami, W., Boher, M., Michard, A. and Albarede, F. (1990) A Major 2.1 Ga Event of Mafic Magmatism in West Africa: An Early Stage of Crustal Accretion. *Journal of Geophysical Research*: *Solid Earth*, **95**, 17605-17629. https://doi.org/10.1029/jb095ib11p17605

[2] Boher, M., Abouchami, W., Michard, A., Albarede, F. and Arndt, N.T. (1992) Crustal Growth in West Africa at 2.1 Ga. *Journal of Geophysical Research*: *Solid Earth*, **97**, 345-369. https://doi.org/10.1029/91jb01640

[3] Feybesse, J. and Milési, J. (1994) The Archaean/Proterozoic Contact Zone in West Africa: A Mountain Belt of Décollement Thrusting and Folding on a Continental Margin Related to 2.1 Ga Convergence of Archaean Cratons? *Precambrian Research*, **69**, 199-227. https://doi.org/10.1016/0301-9268(94)90087-6

[4] Block, S., Jessell, M., Aillères, L., Baratoux, L., Bruguier, O., Zeh, A., *et al*. (2016) Lower Crust Exhumation during Paleoproterozoic (Eburnean) Orogeny, NW Ghana, West African Craton: Interplay of Coeval Contractional Deformation and Extensional Gravitational Collapse. *Precambrian Research*, **274**, 82-109. https://doi.org/10.1016/j.precamres.2015.10.014

[5] Chudasama, B., Porwal, A., Kreuzer, O.P. and Butera, K. (2016) Geology, Geodynamics and Orogenic Gold Prospectivity Modelling of the Paleoproterozoic Kumasi Basin, Ghana, West Africa. *Ore Geology Reviews*, **78**, 692-711. https://doi.org/10.1016/j.oregeorev.2015.08.012

[6] Chardon, D., Bamba, O. and Traoré, K. (2020) Eburnean Deformation Pattern of Burkina Faso and the Tectonic Significance of Shear Zones in the West African Craton. *BSGF—Earth Sciences Bulletin*, **191**, Article No. 2. https://doi.org/10.1051/bsgf/2020001

[7] Junner, N.R. (1940) Geology of the Gold Coast and Western Togoland. *Gold Coast Geological Survey Bulletin*, No. 11, 40.

[8] Gasquet, D., *et al*. (2003) Transcurrent Tectonics and Polycyclic Evolution in the Pan-African Domain of the Moroccan Anti-Atlas. *Precambrian Research*, **120**, 263-290.

[9] Kitson, A.F. (1928) Provisional Geological Map of the Gold Coast and Western to Goland, with Brief Descriptive Notes Thereon. Benham & Co. Ltd., 13.

[10] Leube, A., Hirdes, W., Mauer, R. and Kesse, G.O. (1990) The Early Proterozoic Birimian Supergroup of Ghana and Some Aspects of Its Associated Gold Mineralization. *Precambrian Research*, **46**, 139-165. https://doi.org/10.1016/0301-9268(90)90070-7

[11] Baratoux, L., Metelka, V., Naba, S., Jessell, M.W., Grégoire, M. and Ganne, J. (2011) Juvenile Paleoproterozoic Crust Evolution during the Eburnean Orogeny (~2.2 - 2.0 Ga), Western Burkina Faso. *Precambrian Research*, **191**, 18-45. https://doi.org/10.1016/j.precamres.2011.08.010

[12] Metelka, V., Baratoux, L., Naba, S. and Jessell, M.W. (2011) A Geophysically Constrained Litho-Structural Analysis of the Eburnean Greenstone Belts and Associated Granitoid Domains, Burkina Faso, West Africa. *Precambrian Research*, **190**, 48-69. https://doi.org/10.1016/j.precamres.2011.08.002

[13] Doumbia, S., Pouclet, A., Kouamelan, A., Peucat, J.J., Vidal, M. and Delor, C. (1998) Petrogenesis of Juvenile-Type Birimian (Paleoproterozoic) Granitoids in Central Côte-d'Ivoire, West Africa: Geochemistry and Geochronology. *Precambrian Research*, **87**, 33-63. https://doi.org/10.1016/s0301-9268(97)00201-5

[14] Feybesse, J., Billa, M., Guerrot, C., Duguey, E., Lescuyer, J., Milesi, J., *et al*. (2006) The Paleoproterozoic Ghanaian Province: Geodynamic Model and Ore Controls, Including Regional Stress Modeling. *Precambrian Research*, **149**, 149-196. https://doi.org/10.1016/j.precamres.2006.06.003

[15] Hirdes, W., Davis, W.D. and Lüdtke, G. (1996) Geochemical and Geochronological Constraints on Evolution of Birimian Greenstone Belts of Ghana, West Africa. *Precambrian Research*, **80**, 25-48.

[16] Dewey, J.F. (2002) Transtension in Arcs and Orogens. *International Geology Review*, **44**, 402-439. https://doi.org/10.2747/0020-6814.44.5.402

[17] Castaing, C., *et al*. (2003) Notice explicative de la carte géologique et minière du Burkina Faso à 1/1 000 000. BRGM, 1-147.

[18] Grenholm, M., Jessell, M. and Thébaud, N. (2019) A Geodynamic Model for the Paleoproterozoic (ca. 2.27-1.96 Ga) Birimian Orogen of the Southern West African Craton—Insights into an Evolving Accretionary-Collisional Orogenic System. *Earth-*

Science Reviews, **192**, 138-193. https://doi.org/10.1016/j.earscirev.2019.02.006

[19] Arnould, A. (1961) Étude géologique des migmatites et des granites précambriens du Nord-Est de la Côte d'Ivoire et de la Haute-Volta méridionale. FeniXX réédition numérique (Technip), 175.

[20] Egal, E., Thiéblemont, D., Lahondère, D., Guerrot, C., Costea, C.A., Iliescu, D., *et al*. (2002) Late Eburnean Granitization and Tectonics along the Western and Northwestern Margin of the Archean Kénéma-Man Domain (Guinea, West African Craton). *Precambrian Research*, **117**, 57-84. https://doi.org/10.1016/s0301-9268(02)00060-8

[21] Lompo, M. (2010) Geodynamic Evolution of the West African Craton and Its Bearing on Gold Mineralization. *Mineralium Deposita*, **44**, 489-511.

[22] Bonhomme, M. (1962) Contribution à l'étude géochronologique de la plate-forme de l'Ouest Africain. Imprimerie Louis-Jean, 62.

[23] Allibone, A. (2002) Timing and Structural Controls on Gold Mineralization at the Bogoso Gold Mine, Ghana, West Africa. *Economic Geology*, **97**, 949-969. https://doi.org/10.2113/97.5.949

[24] Bessoles, B. (1977) Géologie de l'Afrique. Le craton Ouest Africain. BRGM, 403.

[25] Pouclet, A., *et al*. (2006) The Metallogenic Role of Granites in Birimian Gold Mineralization in West Africa: A Reappraisal. *Ore Geology Reviews*, **28**, 187-210.

[26] Naba, S., *et al*. (2004) Petrogenesis of Paleoproterozoic Volcanic Rocks of the Youga Gold District, Burkina Faso: Implications for Gold Mineralization. *Journal of African Earth Sciences*, **39**, 1-22.

[27] Yameogo, O.A., Naba, S. and Traore, S.A. (2020) Caractères pétrographiques et Géochimiques des granitoïdes de la région de Dori au Nord-Est du Burkina Faso, Craton Ouest Africain. *Afrique Science*, **16**, 375-395.

[28] Soumaila, A. (2000) Etude structurale, pétrographique et géochimique de la ceinture birimienne de Diagorou-Darbani, Liptako, Niger occidental (Afrique de l'Ouest). Master's Thesis, Université de Franche-Comté.

[29] Vegas, N., Naba, S., Bouchez, J.L. and Jessell, W.M. (2008) Structure and Emplacement of Granite Plutons in the Paleoproterozoic Crust of Eastern Burkina Faso: Rheological Implications. *International Journal of Earth Sciences*, **97**, 1165-1180.

[30] Traore, A.S., Naba, S., Kagambega, N., Lompo, M., Baratoux, L. and Ganne J. (2011) Mise en place tardiorogenique de la syénite de wayen (Burkina Faso, Afrique de l'Ouest). *Journal des Sciences et Technologies*, **9**, 33-48.

[31] Sawadogo, S. (2017) Les plutons granitiques de la ceinture de Djibo au Nord du Burkina Faso (Afrique de l'ouest): Mécanismes de mise en place et implications dans l'évolution géodynamique de la ceinture. Master's Thesis, Université Ouaga I Professeur Joseph Ki-Zerbo.

[32] Deng, Q., Wu, D., Zhang, P. and Chen, S. (1986) Structure and Deformational Character of Strike-Slip Fault Zones. *pure and applied geophysics*, **124**, 203-223. https://doi.org/10.1007/bf00875726

[33] Dewey, J.F. (1988) Extensional Collapse of Orogens. *Tectonics*, **7**, 1123-1139. https://doi.org/10.1029/tc007i006p01123

[34] Milési, J., Ledru, P., Feybesse, J., Dommanget, A. and Marcoux, E. (1992) Early Proterozoic Ore Deposits and Tectonics of the Birimian Orogenic Belt, West Africa. *Precambrian Research*, **58**, 305-344. https://doi.org/10.1016/0301-9268(92)90123-6

[35] Lebrun, E., Thébauda, N., Miller, J., Ulrichb, S., Bourget, J. and Terblanche, O. (2016) Geochronology and Lithostratigraphy of the Siguiri District: Implications for Gold Mineralization in the Siguiri Basin (Guinea, West Africa). *Precambrian Research*,

274, 136-160.

[36] Salmi, S., Errami, E., Jouhari, A., El Kabouri, J., Ennih, N., Outaaoui, O., *et al*. (2024) Constraints of the Regional Deformation on the Hydrothermal Veins in Ousdrat and Aït Ahmane Ore Deposits (Bou Azzer-El Graara Inlier, Central Anti-Atlas, Morocco): Implications for Mineral Exploration. *Journal of African Earth Sciences*, **220**, Article ID: 105441. https://doi.org/10.1016/j.jafrearsci.2024.105441

[37] Salmi, S., Errami, E., Jouhari, A., Lentz, D.R., Essalhi, M., Outaaoui, O., *et al*. (2025) Quantification of Hydrothermal Alteration in Co-Ni-Rich Mineralized Structures along Fault Segments Crossing the Aït Ahmane and Ousdrat Plutons, Bou Azzer El-Graara Inlier, Central Anti-Atlas: Implications for Genesis and Mineral Exploration. *Journal of Geochemical Exploration*, **273**, Article ID: 107712. https://doi.org/10.1016/j.gexplo.2025.107712

[38] Dabo, M. (2011) Tectonique et minéralisations aurifères dans les formations birimiennes de Frandi-Boboti, boutonnière de Kédougou-Kéniéba, Sénégal. Master's Thesis, Université Rennes 1.

[39] Dabo, M. and Aïfa, T. (2011) Late Eburnean Deformation in the Kolia-Boboti Sedimentary Basin, Kédougou-Kéniéba Inlier, Sénégal. *Journal of African Earth Sciences*, **60**, 106-116. https://doi.org/10.1016/j.jafrearsci.2011.02.005

[40] Pons, J., Liégeois, P.J. and Tchaméni, R. (1995) The Pan-African Belt of Central Africa Revisited: New Geochronological and Geochemical Data. *Precambrian Research*, **69**, 243-276.

[41] Baratoux, L., Metelka, V., Naba, S., Ouiya, P., Siebenaller, L., Jessell, M.W., *et al*. (2015) Tectonic Evolution of the Gaoua Region, Burkina Faso: Implications for Mineralization. *Journal of African Earth Sciences*, **112**, 419-439. https://doi.org/10.1016/j.jafrearsci.2015.10.004

[42] Fontaine, A., Eglinger, A., Ada, K., André-Mayer, A., Reisberg, L., Siebenaller, L., *et al*. (2017) Geology of the World-Class Kiaka Polyphase Gold Deposit, West African Craton, Burkina Faso. *Journal of African Earth Sciences*, **126**, 96-122. https://doi.org/10.1016/j.jafrearsci.2016.11.017

[43] Hein, K.A.A. (2010) Succession of Structural Events in the Goren Greenstone Belt (Burkina Faso): Implications for West African Tectonics. *Journal of African Earth Sciences*, **56**, 83-94. https://doi.org/10.1016/j.jafrearsci.2009.06.002

[44] Nikiema, S., Benkhelil, J., Corsini, M., Bourges, F., Dia, A. and Maurin, J.C. (1993) Tectonique trancurrente eburnéenne au sein du Craton-Ouest Africain. Exemple du sillon de Djibo (Burkina Faso). *Comptes Rendus de l'Académie des Sciences—Series III—Sciences de la Vie*, **II**, 661-668.

[45] Sawadogo, S., Yaméogo, O.A. and Naba, S. (2021) Caracterisation des structures de deformation eburneennes dans la ceinture de roches vertes et les granitoïdes de la region de zorgho (centre du Burkina Faso). *Annales de l'Université Joseph KI-ZERBO—Série C*, **19**, 24.

[46] Tshibubudze, A., Hein, K.A.A. and McCuaig, T.C. (2015) The Relative and Absolute Chronology of Strato-Tectonic Events in the Gorom-Gorom Granitoid Terrane and Oudalan-Gorouol Belt, Northeast Burkina Faso. *Journal of African Earth Sciences*, **112**, 382-418. https://doi.org/10.1016/j.jafrearsci.2015.04.008

[47] Vernon, H.R. (2000) Review of Microstructural Evidence of Magmatic and Solid-State Flow. *Visual Geosciences*, **5**, 1-23.

[48] Affaton, P., Tairou, M., Tossa, C., Chala, D. and Kwekam, M. (2013) Premières Données Microstructurales sur le Complexe Granito-Migmatitique de la Région De Nikki, Nebénin. *Global Journal of Geological Sciences*, **11**, 13-26. https://doi.org/10.4314/gjgs.v11i1.2